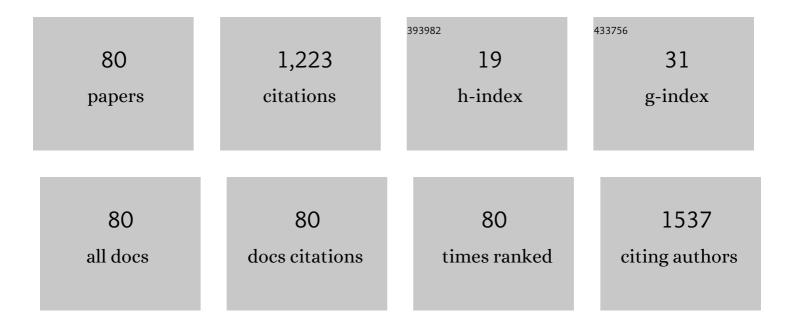
Tae-Sik Yoon

List of Publications by Year in descending order

Source: https://exaly.com/author-pdf/8072360/publications.pdf Version: 2024-02-01



TAE-SIK YOON

#	Article	IF	CITATIONS
1	Interface state-dependent synaptic characteristics of Pt/CeO2/Pt memristors controlled by post-deposition annealing. Materials Science in Semiconductor Processing, 2022, 147, 106718.	1.9	6
2	Improvement of forming-free threshold switching reliability of CeO2-based selector device by controlling volatile filament formation behaviors. APL Materials, 2022, 10, .	2.2	9
3	Electroforming-free threshold switching of NbO _{<i>x</i>} –based selector devices by controlling conducting phases in the NbO _{<i>x</i>} layer for the application to crossbar array architectures. RSC Advances, 2022, 12, 18547-18558.	1.7	3
4	Nonvolatile memory characteristics associated with oxygen ion exchange in thin-film transistors with indium-zinc oxide channel and HfO2-x gate oxide. Materials Today Advances, 2022, 15, 100264.	2.5	3
5	Wide range modulation of synaptic weight in thin-film transistors with hafnium oxide gate insulator and indium-zinc oxide channel layer for artificial synapse application. Nanoscale, 2021, 13, 11370-11379.	2.8	5
6	Analog Memristive Characteristics of Square Shaped Lanthanum Oxide Nanoplates Layered Device. Nanomaterials, 2021, 11, 441.	1.9	4
7	CsPbBr ₃ Perovskite Quantum Dot Lightâ€Emitting Diodes Using Atomic Layer Deposited Al ₂ O ₃ and ZnO Interlayers. Physica Status Solidi - Rapid Research Letters, 2020, 14, 1900573.	1.2	19
8	Strain-Induced Photocurrent Enhancement in Photodetectors Based on Nanometer-Thick ZnO Films on Flexible Polydimethylsiloxane Substrates. ACS Applied Nano Materials, 2020, 3, 10922-10930.	2.4	11
9	Effect of the Bilayer Period of Atomic Layer Deposition on the Growth Behavior and Electrical Properties of the Amorphous In–Zn–O Film. ACS Applied Materials & Interfaces, 2020, 12, 39372-39380.	4.0	3
10	Nonvolatile Memory and Artificial Synaptic Characteristics in Thinâ€Film Transistors with Atomic Layer Deposited HfOx Gate Insulator and ZnO Channel Layer. Advanced Electronic Materials, 2020, 6, 2000412.	2.6	13
11	Enhanced Brightness and Device Lifetime of Quantum Dot Lightâ€Emitting Diodes by Atomic Layer Deposition. Advanced Materials Interfaces, 2020, 7, 2000343.	1.9	12
12	Lightâ€Emitting Diodes: Enhanced Brightness and Device Lifetime of Quantum Dot Lightâ€Emitting Diodes by Atomic Layer Deposition (Adv. Mater. Interfaces 12/2020). Advanced Materials Interfaces, 2020, 7, 2070067.	1.9	1
13	Effect of nitrogen-doping on drain current modulation characteristics of an indium-gallium-zinc oxide thin-film transistor. Nanotechnology, 2020, 31, 265201.	1.3	4
14	CsPbBr ₃ Perovskite Quantum Dot Lightâ€Emitting Diodes Using Atomic Layer Deposited Al ₂ O ₃ and ZnO Interlayers. Physica Status Solidi - Rapid Research Letters, 2020, 14, 2070012.	1.2	3
15	Enhancement of cortisol measurement sensitivity by laser illumination for AlGaN/GaN transistor biosensor. Biosensors and Bioelectronics, 2020, 159, 112186.	5.3	23
16	Compliance Current-Controlled Conducting Filament Formation in Tantalum Oxide-Based RRAM Devices with Different Top Electrodes. ACS Applied Electronic Materials, 2020, 2, 1154-1161.	2.0	55
17	Post-annealing temperature-dependent electrical properties of thin-film transistors with a ZnO channel and HfOx gate insulator deposited by atomic layer deposition. Semiconductor Science and Technology, 2020, 35, 075013.	1.0	5
18	A Pt/ITO/CeO2/Pt memristor with an analog, linear, symmetric, and long-term stable synaptic weight modulation. APL Materials, 2019, 7, 071113.	2.2	23

#	Article	IF	CITATIONS
19	Nonvolatile reversible capacitance changes through filament formation in a floating-gate metal-oxide-semiconductor capacitor with Ag/CeOx/Pt/HfOx/n-Si structure. Applied Physics Letters, 2019, 115, 072106.	1.5	8
20	Analog Memristive Characteristics of Mesoporous Silica–Titania Nanocomposite Device Concurrent with Selection Diode Property. ACS Applied Materials & Interfaces, 2019, 11, 36807-36816.	4.0	10
21	Reversible capacitance changes in the MOS capacitor with an ITO/CeO2/p-Si structure. Journal of Alloys and Compounds, 2019, 786, 655-661.	2.8	16
22	Resistive switching characteristics of ZnO nanoparticles layer-by-layer assembly based on cortisol and its antibody immune binding. Journal of Industrial and Engineering Chemistry, 2019, 78, 66-72.	2.9	3
23	Reversible transition of volatile to non-volatile resistive switching and compliance current-dependent multistate switching in IGZO/MnO RRAM devices. Applied Physics Letters, 2019, 114, .	1.5	60
24	Effects of gamma irradiation on the electrical characteristics of trench-gate non-punch-through insulated gate bipolar transistor. Semiconductor Science and Technology, 2019, 34, 065022.	1.0	2
25	Single- and double-gate synaptic transistor with TaO <i> _x </i> gate insulator and IGZO channel layer. Nanotechnology, 2019, 30, 025203.	1.3	26
26	Multistate resistive switching characteristics of ZnO nanoparticles embedded polyvinylphenol device. Journal of Industrial and Engineering Chemistry, 2018, 64, 85-89.	2.9	15
27	Tri-state resistive switching characteristics of MnO/Ta ₂ O ₅ resistive random access memory device by a controllable reset process. Journal Physics D: Applied Physics, 2018, 51, 225102.	1.3	5
28	Synaptic characteristics with strong analog potentiation, depression, and short-term to long-term memory transition in a Pt/CeO2/Pt crossbar array structure. Nanotechnology, 2018, 29, 265204.	1.3	10
29	Resistive switching characteristics of Ag/MnO/CeO 2 /Pt heterostructures memory devices. Microelectronic Engineering, 2018, 189, 28-32.	1.1	16
30	Resistive switching characteristics of manganese oxide thin film and nanoparticle assembly hybrid devices. Japanese Journal of Applied Physics, 2018, 57, 06HC03.	0.8	20
31	Synaptic behaviors of thin-film transistor with a Pt/HfO <i>_x</i> /n-type indium–gallium–zinc oxide gate stack. Nanotechnology, 2018, 29, 295201.	1.3	4
32	Analog reversible nonvolatile memcapacitance in metal-oxide-semiconductor memcapacitor with ITO/HfOx/Si structure. Applied Physics Letters, 2018, 113, .	1.5	27
33	Synaptic transistor with a reversible and analog conductance modulation using a Pt/HfOx/n-IGZO memcapacitor. Nanotechnology, 2017, 28, 225201.	1.3	20
34	A memristor crossbar array of titanium oxide for non-volatile memory and neuromorphic applications. Semiconductor Science and Technology, 2017, 32, 065014.	1.0	43
35	Forming-free resistive switching characteristics of Ag/CeO ₂ /Pt devices with a large memory window. Semiconductor Science and Technology, 2017, 32, 055006.	1.0	18
36	Artificial synaptic characteristics with strong analog memristive switching in a Pt/CeO ₂ /Pt structure. Nanotechnology, 2017, 28, 285203.	1.3	38

#	Article	IF	CITATIONS
37	Resistive Switching Characteristics of Tantalum Oxide and Titanium Oxide Heterojunction Devices. Journal of Nanoscience and Nanotechnology, 2017, 17, 7150-7154.	0.9	10
38	Resistive Switching Characteristics in MnO Nanoparticle Assembly and Ag ₂ Se Thin Film Devices. Journal of Nanoscience and Nanotechnology, 2017, 17, 7189-7193.	0.9	7
39	Solution Processed Hafnium Oxide Doped Siloxane Dielectrics for a Thin Film Transistor with Reduced Graphene Oxide Channel on Flexible Substrate. Journal of Nanoscience and Nanotechnology, 2017, 17, 7423-7428.	0.9	1
40	Memcapacitive characteristics in reactive-metal (Mo, Al)/HfOX/n-Si structures through migration of oxygen by applied voltage. Applied Physics Letters, 2016, 108, .	1.5	17
41	The <inline-formula> <tex-math notation="LaTeX">\$gamma \$ </tex-math> </inline-formula>-Fe₂O₃Nanoparticle Assembly-Based Memristor Ratioed Logic and Its Optical Tuning. IEEE Electron Device Letters, 2016, 37, 986-989.</inline-formula>	2.2	5
42	Resistive switching of in situ polymerized polystyrene matrix copolymerized with alkanedienyl passivated Si nanoparticles. Microelectronic Engineering, 2015, 136, 26-30.	1.1	10
43	Analog Memristive and Memcapacitive Characteristics of Pt-Fe ₂ O ₃ Core-Shell Nanoparticles Assembly on p ⁺ -Si Substrate. IEEE Nanotechnology Magazine, 2015, 14, 798-805.	1.1	19
44	Resistive switching characteristics of TiO2 thin films with different electrodes. Journal of the Korean Physical Society, 2015, 67, 936-940.	0.3	5
45	Electrical charging characteristics of Au NPs embedded by sequence specific complementary DNA hybridization in metal-pentacene-insulator-silicon device. Biochip Journal, 2014, 8, 275-281.	2.5	9
46	Voltage-dependent resistive switching characteristics in mixed layer consisting of γ-Fe ₂ O ₃ and Pt-Fe ₂ O ₃ core-shell nanoparticles. Applied Physics Letters, 2014, 104, 093514.	1.5	8
47	Robust ZnO nanoparticle embedded memory device using vancomycin conjugate and its biorecognition for electrical charging node. Biosensors and Bioelectronics, 2014, 56, 33-38.	5.3	16
48	Affinity Characteristics of Histone-Derived Peptide Layer by Memory Charging Effect Using Chromatin Protein Conjugated Gold Nanoparticles. Science of Advanced Materials, 2014, 6, 2478-2482.	0.1	2
49	Tunable threshold resistive switching characteristics of Pt–Fe ₂ O ₃ core–shell nanoparticleassembly by space charge effect. Nanoscale, 2013, 5, 772-779.	2.8	36
50	Analog and bipolar resistive switching in pn junction of n-type ZnO nanowires on p-type Si substrate. Journal of Applied Physics, 2013, 114, 064502.	1.1	19
51	Digital versus analog resistive switching depending on the thickness of nickel oxide nanoparticle assembly. RSC Advances, 2013, 3, 20978.	1.7	53
52	Non-volatile nano-floating gate memory with Pt-Fe2O3 composite nanoparticles and indium gallium zinc oxide channel. Journal of Nanoparticle Research, 2013, 15, 1.	0.8	10
53	Morphological dependence of hydrothermally synthesized ZnO nanowires on synthesis temperature and molar concentration. Physica Status Solidi (A) Applications and Materials Science, 2013, 210, 1448-1453.	0.8	5
54	Multimode threshold and bipolar resistive switching in bi-layered Pt-Fe2O3 core-shell and Fe2O3 nanoparticle assembly. Applied Physics Letters, 2013, 102, .	1.5	23

#	Article	IF	CITATIONS
55	Organic memory device with self-assembly monolayered aptamer conjugated nanoparticles. Applied Physics Letters, 2013, 103, .	1.5	10
56	Investigation of analog memristive switching of iron oxide nanoparticle assembly between Pt electrodes. Journal of Applied Physics, 2013, 114, 224505.	1.1	24
57	Attachment of FePt-Fe2 O3 core-shell nanoparticles on carbon nanotubes and their electrical-transport characteristics. Physica Status Solidi (A) Applications and Materials Science, 2013, 210, 2622-2627.	0.8	1
58	Organic memory device with polyaniline nanoparticles embedded as charging elements. Applied Physics Letters, 2012, 100, 163301.	1.5	31
59	Resistive Switching Characteristics of Core-Shell Nanoparticles of Metal-Oxide on Flexible Substrate. ECS Transactions, 2011, 41, 483-488.	0.3	1
60	Nanocrystal floating gate memory with solution-processed indium-zinc-tin-oxide channel and colloidal silver nanocrystals. Semiconductor Science and Technology, 2011, 26, 125021.	1.0	6
61	Selective Incorporation of Colloidal Nanocrystals in Nanopatterned SiO[sub 2] Layer for Nanocrystal Memory Device. Electrochemical and Solid-State Letters, 2010, 13, K19.	2.2	5
62	Controlling dislocation positions in silicon germanium (SiGe) buffer layers by local oxidation. Thin Solid Films, 2010, 518, S217-S221.	0.8	0
63	Effects on Annealing Temperature for Solution-Processed IZTO TFTs by Nitrogen Incorporation. Electrochemical and Solid-State Letters, 2010, 13, H419.	2.2	18
64	Electrical charging of Au nanoparticles embedded by streptavidin-biotin biomolecular binding in organic memory device. Applied Physics Letters, 2010, 97, .	1.5	18
65	Vertically and Laterally Self-Aligned Double Layer of Nanocrystals in Nanopatterned Dielectric Layer for Nanocrystal Floating Gate Memory Device. Electrochemical and Solid-State Letters, 2010, 13, H366.	2.2	3
66	Use of fluorine-doped tin oxide instead of indium tin oxide in highly efficient air-fabricated inverted polymer solar cells. Applied Physics Letters, 2010, 96, .	1.5	109
67	Completely Filling Anodic Aluminum Oxide with Maghemite Nanoparticles by Dip Coating and Their Magnetic Properties. Electrochemical and Solid-State Letters, 2009, 12, K59.	2.2	17
68	Electrical properties of charging effect in Au nanoparticle memory device. Materials Research Society Symposia Proceedings, 2009, 1207, 1.	0.1	0
69	Colloidal Nanoparticle-Layer Formation Through Dip-Coating: Effect of Solvents and Substrate Withdrawing Speed. Journal of the Electrochemical Society, 2009, 156, K86.	1.3	27
70	Improvement of dynamic characteristics of polydimethylsiloxane based microvalve. Microsystem Technologies, 2009, 15, 607-609.	1.2	2
71	The effect of excess surfactants on the adsorption of iron oxide nanoparticles during a dip-coating process. Journal of Nanoparticle Research, 2009, 11, 831-839.	0.8	16
72	Study of growth behaviour and microstructure of epitaxially grown selfâ€assembled Ge quantum dots on nanometerâ€scale patterned SiO ₂ /Si(001) substrates. Physica Status Solidi (B): Basic Research, 2009, 246, 721-724.	0.7	5

#	Article	IF	Citations
73	Assembly of Colloidal Nanoparticles into Anodic Aluminum Oxide Templates by Dip-Coating Process. IEEE Nanotechnology Magazine, 2009, 8, 707-712.	1.1	12
74	Nucleation kinetics of Ru on silicon oxide and silicon nitride surfaces deposited by atomic layer deposition. Journal of Applied Physics, 2008, 103, .	1.1	69
75	Surface roughness and dislocation distribution in compositionally graded relaxed SiGe buffer layer with inserted-strained Si layers. Applied Physics Letters, 2005, 87, 012104.	1.5	19
76	Ge-rich Si[sub 1â^'x]Ge[sub x] nanocrystal formation by the oxidation of an as-deposited thin amorphous Si[sub 0.7]Ge[sub 0.3] layer. Journal of Vacuum Science & Technology an Official Journal of the American Vacuum Society B, Microelectronics Processing and Phenomena, 2002, 20, 631.	1.6	10
77	Ge-rich Si1-XGeX Nanocrystal Formation by the Oxidation of As-Deposited Thin Amorphous Si0.7Ge0.3 Layer. Materials Research Society Symposia Proceedings, 2002, 727, 1.	0.1	0
78	High spatial density nanocrystal formation using thin layer of amorphous Si0.7Ge0.3 deposited on SiO2. Journal of Applied Physics, 2000, 87, 2449-2453.	1.1	20
79	Si/sub 0.7/Ge/sub 0.3/ Quantum Dot Formation by Interface Agglomeration. , 1998, , .		0
80	Programming dynamics of a single electron memory cell with a high-density SiGe nanocrystal array at room temperature. , 0, , .		2